Focused-Ion-Beam Nanofabrication of Near-Infrared Magnetic Metamaterials**

By *Christian Enkrich*, *Fábian Pérez-Willard*, *Dagmar Gerthsen*, *Jiangfeng Zhou*, *Thomas Koschny*, *Costas M. Soukoulis*, *Martin Wegener*, and *Stefan Linden**

Natural substances exhibit a negligible magnetic response at optical frequencies, that is, their magnetic permeability is unity ($\mu = 1$). Consequently, their optical properties are solely determined by the electronic response characterized by the permittivity ε. Given that, the work of Veselago[1] on the electrodynamics of substances with simultaneously negative ε and μ, which leads to a negative index of refraction, n, (left-handed materials), appeared to be rather academic at the time. The situation totally changed in 1999, when Pendry et al. proposed to utilize an array of subwavelength split-ring resonators (SRRs) to create a metamaterial with negative magnetic permeability.[2] Only two years later, Veselago's vision was realized and an artificial structure with negative index of refraction operating at a frequency of around 10 GHz (3 cm wavelength) was demonstrated experimentally.[3] Recently, metamaterials have been realized with a magnetic response around 1 THz (300 μm wavelength),[4] 6 THz (50 μm wavelength),[5] 65 THz (4.6 μm wavelength),[6] and 100 THz (3.2 μm wavelength).[7]

SRRs form the "heart" of most magnetic metamaterials presented in experiments so far. SSRs can be viewed as a circuit formed by the inductance L of a coil with a single metallic winding, and a capacitance C brought about by the ends of the wire. In the following, such a circuit will be referred to as an LC circuit. The oscillating current in the LC circuit leads to a magnetic moment perpendicular to the plane shown in Figure 1A. It is known that the LC resonance frequency scales inversely with the lateral size of the SRR, provided that all parameters are simultaneously scaled down and provided that the resonance frequency does not come close to the metal plasma frequency. For example, for the structures described by Linden et al.[7] (schematically shown in Fig. 1A) with a magnetic resonance wavelength of 3 μm, the minimum feature size (gap width) is 70 nm. Scaling to 1.5 μm resonance wavelength would translate into 35 nm minimum feature size, which is possible for a single SRR but not easy to obtain for arrays containing more than thousand *identical* SRRs (Fig. 2). Thus, alternative designs with short resonance wavelengths and fewer intricate fine details would be desirable. The examples shown in Figures 1B,C should be easily accessible with state-of-the-art nanofabrication tools, e.g., by electron-beam lithography or focused-ion-beam (FIB) writing. However, it is not a priori clear how appropriate these designs are for magnetic metamaterials. For electron-beam lithography, SRR arrays of this sort require time-consuming dose tests and processing steps, leading to relatively long overall fabrication times. In contrast, we show that complete structures can be fabricated via FIB writing in times as short as 20 min (rapid prototyping). Thus, we have fabricated a large variety of different structures via FIB writing. An example of an SRR array is illustrated in Figure 2.

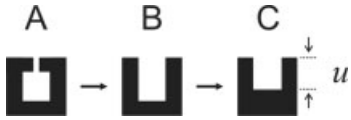

Figure 1. Schematic representation of three different SRR designs. For $u = 0$ one obtains a square metal nanoparticle.

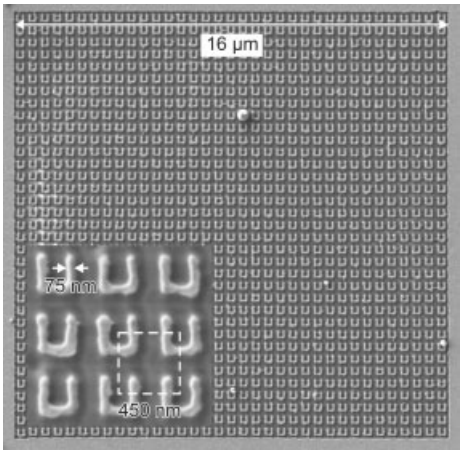

Figure 2. Electron microscope image of a 16 μm × 16 μm array of SRRs fabricated using FIB writing. Inset: a magnified image.

[*] Dr. S. Linden, Prof. M. Wegener
Institut für Nanotechnologie
Forschungszentrum Karlsruhe in der Helmholtz-Gemeinschaft
D-76021 Karlsruhe (Germany)
E-mail: stefan.linden@physik.uni-karlsruhe.de
C. Enkrich, Prof. M. Wegener
Institut für Angewandte Physik
Universität Karlsruhe (TH)
D-76131 Karlsruhe (Germany)
Dr. F. Pérez-Willard, Prof. D. Gerthsen
Laboratorium für Elektronenmikroskopie
Universität Karlsruhe (TH)
D-76131 Karlsruhe (Germany)
J. F. Zhou, Dr. T. Koschny, Prof. C. M. Soukoulis
Ames Laboratory and Department of Physics and Astronomy
Iowa State University
Ames, IA 50011 (USA)
Prof. C. M. Soukoulis
Institute of Electronic Structure and Laser
FORTH and Department of Materials Science and Technology
71110 Heraklion, Crete (Greece)

[**] We acknowledge the support by the Center for Functional Nanostructures (CFN) of the Deutsche Forschungsgemeinschaft (DFG) within subproject A.1.5. The research of M. W. is further supported by the DFG-Leibniz award 2000 and that of C. M. S. by the Alexander von Humboldt Senior-Scientist Award 2002, by Ames Laboratory (W-7405-Eng-82), by EU-DALHM and DARPA (MDA 972-01-2-0016).

 DOI: 10.1002/adma.200500804

ADVANCED MATERIALS

Figure 3 summarizes selected examples of measured normal-incidence optical transmission spectra. The three different rows correspond to three different SRR designs (as indicated by the electron micrographs in the insets). Here, the only design parameter that has been changed is the depth, u, of the "U" (see Fig. 1). The two columns correspond to two linear polarizations with respect to the SRR (see top). In the left-hand-side (LHS) column, the electric field (arrow) of the incident light can couple to the capacitance, in the right-hand-side (RHS) column it cannot. Thus, for normal incidence, a magnetic resonance is only expected to occur in the LHS column.[7,8] Indeed, on the LHS two resonances appear in the measured spectra, while only one short-wavelength resonance is visible in the RHS column. Thus, the long-wavelength resonance in the LHS column is the magnetic dipole (or LC circuit) resonance. The short-wavelength transmission minimum corresponds to the electric-dipole (or Mie) resonance. This overall qualitative behavior has already been observed and discussed.[7] Note that the Mie resonance wavelength is similar for the three different SRR designs, whereas the magnetic resonance wavelength can be tuned by almost a factor of two—without significant reduction of the minimum feature size.

In order to further strengthen our above qualitative interpretation, we have compared the measurements with theory. In these calculations, the actual geometrical parameters taken from the corresponding electron micrographs (see white lines in Fig. 3) have been used. Numerical results are shown in Figure 4, which can be directly compared with the experiment (Fig. 3). The overall qualitative agreement is very good; remaining discrepancies are likely a result of fabrication tolerances of the SRR in the array (see Fig. 2). Importantly, the absolute spectral positions of the peaks are reproduced well. This is also true for other values of u. The measured and calculated resonance positions are summarized in Figure 5.

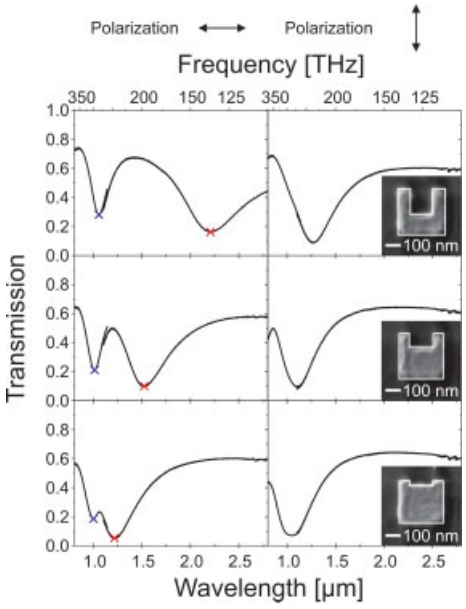

Figure 3. Measured transmission spectra. The three different rows correspond to three different SRR designs that differ only in the depth u of the "U" (see electron microscope images in the insets, from top to bottom: u = 160, 85, and 30 nm). The two columns correspond to two linear polarizations with respect to the SRR (see top). The blue and red crosses correspond to the spectral positions of the electric and magnetic resonances, respectively, summarized in Figure 5.

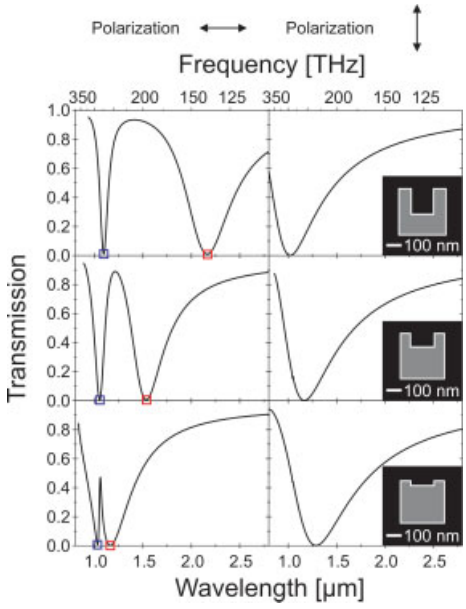

Figure 4. Calculated transmission spectra corresponding to the experiments shown in Figure 3, for the depths u = 160, 85, and 30 nm (from top to bottom). The blue and red squares correspond to the spectral positions of the electric and magnetic resonances, respectively, summarized in Fig. 5.

It is known that a negative permeability is not to be expected for normal incidence, whereas it can and does occur for propagation of light in the SRR array plane. For the latter

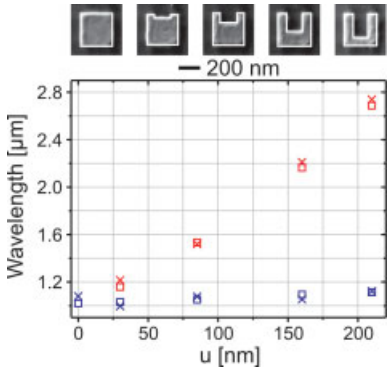

Figure 5. Measured (crosses) and calculated (squares) spectral positions of the magnetic resonance (red) and the electric resonance (blue) as a function of the depth u (from left to right: u = 0, 30, 85, 160, and 210 nm). The corresponding raw data have been exemplified in Figs. 3,4. The corresponding five SRR designs are depicted at the top.

propagation geometry, we have performed the retrieval[7,9] of the effective magnetic permeability μ and the effective electric permittivity ε on the basis of calculated optical spectra. Generally, the shape of the retrieved spectra of ε and μ are similar to those, e.g., shown in Figure 4 of our recent publication.[7] Thus, the retrieved spectra are not shown here. For the SRR parameters of the first row of Figure 4 we find a resonance in μ with $\mu < 0$ around a wavelength of 2.4 μm. For the SRR parameters of the second row of Figure 4 we find a resonance in μ around 1.7 μm with reduced oscillator strength, thus $\mu > 0$, but still with a negative magnetic susceptibility. The oscillator strength is yet further reduced for the SRR parameters of the third row of Figure 4, corresponding to a magnetic resonance around a wavelength of 1.2 μm.

In conclusion, we have designed and realized a variety of different metamaterials, taking advantage of the rapid prototyping capabilities of FIB nanofabrication. In particular, we have demonstrated a continuous transition from square-shaped metallic pads that exhibit a twofold degenerate Mie (electric dipole) resonance to SRRs with a red-shifted fundamental magnetic-dipole response and one remaining Mie resonance. The retrieval of the corresponding calculated optical spectra reveals a magnetic response with a negative magnetic susceptibility (although $\mu > 0$) at a wavelength of 1.7 μm and a negative permeability (i.e., $\mu < 0$) at a wavelength of 2.4 μm for propagation in the split-ring array plane. Overall, our results show the robustness of the SRR concept. Such robustness is especially important for nanometer-sized SRR arrays where fabrication tolerances are much more of an issue than for microwave structures. Combined with metallic nanowires leading to a negative permittivity, our findings on magnetic split rings pave the road for left-handed metamaterials at telecommunication wavelengths.

Experimental

The starting point of our nanofabrication process is a glass substrate, coated with a 5 nm thin film of indium tin oxide (ITO) and a 20 nm film of gold. The ITO acts as an adhesion promoter and enhances the quality of the gold film. Both films are deposited by electron-beam evaporation under high vacuum (10^{-4} Pa). The FIB writing corresponds to an inverse process in the sense that the FIB removes material. We use a dual-beam FIB/SEM (scanning electron microscopy) system (Zeiss 1540 XB) and Ga^+ ions accelerated by a voltage of 30 kV. Typical FIB currents are 5 pA, typical exposure doses are 2900 μA s cm^{-2}. Each SRR consists of a square with a side length of 280 nm in which a notch of depth u is cut. The arms of the resulting "U" have a typical width of 75 nm. All structures discussed here consist of an array of 35 × 35 SRRs with a lattice constant of 450 nm (total area of 16 μm × 16 μm). The exposure of one array like the one shown in Figure 2 takes approximately 20 min. Afterwards, the structure can be immediately inspected by the SEM of the dual-beam system and no further post-processing steps are required.

Transmission spectra are measured with a Fourier-transform infrared spectrometer (Bruker Equinox 55, NIR halogen source) combined with an infrared microscope (Bruker Hyperion 1000, 36 × cassegrain lens, numerical aperture NA = 0.5, liquid N_2-cooled InSb detector, infrared polarizer). A circular area with 12 μm diameter is defined by an aperture in the light path of the microscope. The transmission spectra are normalized to the bare substrate, and are taken for two orthogonal linear polarizations of the incident light as indicated on the top of Figure 3. At a wavelength of around 1.1 μm, the optics of the spectrometer have to be changed, which leads to a small discontinuity in the measured curves.

The calculations are performed using the software package CST Microwave Studio. The Drude model is used to describe the metal, i.e., the effective permittivity of metals in the infrared spectral region is given by

$$\varepsilon(\omega) = 1 - (\omega_p^2/[\omega(\omega + i\omega_c)]) \quad (1)$$

where ω_p is the plasma frequency and ω_c is the collision frequency. For bulk gold, we use the parameters $\omega_p = 2\pi \times 2.175 \times 10^{15}$ s^{-1}, $\omega_c = 2\pi \times 6.5 \times 10^{12}$ s^{-1} (identical to our previous choice [7]).

Received: April 20, 2005
Final version: July 15, 2005
Published online: September 13, 2005

[1] V. G. Veselago, *Sov. Phys.—Usp.* **1968**, *10*, 509.
[2] J. B. Pendry, A. J. Holden, D. J. Robbins, W. J. Stewart, *IEEE Trans. Microwave Theory Tech.* **1999**, *47*, 2075.
[3] R. A. Shelby, D. R. Smith, S. Schultz, *Science* **2001**, *292*, 77.
[4] T. J. Yen, W. J. Padilla, N. Fang, D. C. Vier, D. R. Smith, J. B. Pendry, D. N. Basov, X. Zhang, *Science* **2004**, *303*, 1494.
[5] N. Katsarakis, G. Konstantinidis, A. Kostopoulos, R. S. Penciu, T. F. Gundogdu, M. Kafesaki, E. N. Economou, T. Koschny, C. M. Soukoulis, *Opt. Lett.* **2005**, *30*, 1348.
[6] S. Zhang, W. Fan, B. K. Minhas, A. Frauenglass, K. J. Malloy, S. R. J. Brueck, *Phys. Rev. Lett.* **2005**, *94*, 37 402.
[7] S. Linden, C. Enkrich, M. Wegener, J. Zhou, T. Koschny, C. M. Soukoulis, *Science* **2004**, *306*, 1351.
[8] N. Katsarakis, T. Koschny, M. Kafesaki, E. N. Economou, C. M. Soukoulis, *Appl. Phys. Lett.* **2004**, *84*, 2943.
[9] D. R. Smith, S. Schultz, P. Markos, C. M. Soukoulis, *Phys. Rev. B* **2002**, *65*, 195 104.

Characterization of Phase Purity in Organic Semiconductors by Lattice-Phonon Confocal Raman Mapping: Application to Pentacene

By *Aldo Brillante*,* *Ivano Bilotti*, *Raffaele Guido Della Valle*, *Elisabetta Venuti*, *Matteo Masino*, and *Alberto Girlando*

After years of silicon dominance, a new breed of electronic components based on organic semiconductors is emerging, with the goal of making devices that, although not as efficient

[*] Prof. A. Brillante, Dr. I. Bilotti, Prof. R. G. Della Valle, Dr. E. Venuti
Dipartimento di Chimica Fisica e Inorganica
and INSTM-UdR Bologna
University of Bologna
I-40136 Bologna (Italy)
E-mail: aldo.brillante@unibo.it
Dr. M. Masino, Prof. A. Girlando
Dipartimento di Chimica GIAF and INSTM-UdR Parma
University of Parma
I-43100 Parma (Italy)

 DOI: 10.1002/adma.200501350